Hue University Journal of Science: Natural Science
Vol. 128, No. 1B, 49-55, 2019

pISSN 1859-1388
eISSN 2615-9678

STRUCTURE, STABILITY, AND ELECTRONIC PROPERTIES OF SINGLY AND DOUBLY TRANSITION-METAL-DOPED BORON CLUSTERS $B_{14}M$

Nguyen Minh Tam[1,2], My-Phuong Pham-Ho[3]*

[1] Computational Chemistry Research Group, Ton Duc Thang University, Ho Chi Minh City, Vietnam
[2] Faculty of Applied Sciences, Ton Duc Thang University, Ho Chi Minh City, Vietnam
[3] Faculty of Chemical Engineering, Ho Chi Minh City University of Technology, Ho Chi Minh City, Vietnam

Correspondence to Pham Ho My Phuong (email: phmphuong@hcmut.edu.vn)
(Received: 11–8–2019; Accepted: 7–9–2019)

Abstract. An examination of the first-row-transition-metal-doped boron clusters, $B_{14}M$ (M = Sc, Ti, V, Cr, Mn, Fe, Co, Ni, and Cu) in the neutral state, is carried out using DFT quantum chemical calculations. The lowest-energy equilibrium structures of the clusters considered are identified at the TPSSh/ 6-311+G(d) level. The structural patterns of doped species evolve from exohedrally capped quasi-planar structure B_{14} to endohedrally doped double-ring tubular when M is from Sc to Cu. The $B_{14}Ti$ and $B_{14}Fe$ appear as outstanding species due to their enhanced thermodynamic stabilities with larger average binding energies. Their electronic properties can be understood in terms of the density of state.

Keywords: DFT, boron cluster, density of state

1 Introduction

There has been considerable interest in the boron-based clusters as endorsed by a large number of experimental and theoretical investigations in the last decades. This is due to not only their novel physical and chemical properties but also their promising abilities for new technological applications. The structural landscape of small pure boron clusters up to B_{20}, provided by many studies [1], is now clearly determined for both neutral and charged states. It reveals that from the size B_{17}^+ to B_{20}^+, the cations favor a double ring tubular structure [2], whereas anionic and neutral clusters are more stable in the planar form [3, 4] except for the neutral B_{14}. The B_{14} is an extraordinary size during the growth mechanism of small bare boron clusters since it is the smallest all-boron fullerene [5], whereas the dicationic state B_{14}^{2+} was found as the first double-ring (DR) boron cluster [6]. The DR structure emerges from a superposition of two B_k strings leading to a tube B_{2k}. The most stable structure of neutral B_{20}, having the very high stability in comparison with the other isomers, is the most well-known all-boron double ring [7], among the others B_{18}^{2+} [6], B_{22}^{2+} [8], B_{24} [9], etc. For the neutral state of pure boron clusters B_n, however, the DR structures only exist at the sizes $n \geq 20$. The DR tube achieves double aromaticity [10–12] by the classic Hückel $(4N + 2)$ rule for both π electrons (radial electrons) and σ electrons (tangential electrons). It can be thus rationalized for the enhanced stability of the DR structure.

The first-row transition metals, including Sc, Ti, V, Cr, Mn, Fe, Co, Ni, and Cu, which have the unpaired valence electrons $4s^23d^1$, $4s^23d^2$, $4s^23d^3$, $4s^13d^5$, $4s^23d^5$, $4s^23d^6$, $4s^23d^7$, $4s^23d^8$, and $4s^13d^{10}$, respectively, are interesting magnetic elements.

They are expected to become the potential candidates as dopants in clusters due to the interaction between these impurities and host electrons and may alter both electronic and geometrical structures and thus generate the doped cluster possessing the novel physico-chemical properties [13, 14].

Numerous theoretical and experimental studies reported that doping one transition-metal atom on small boron clusters leads to the formation of the wheel-type structures, detected at the sizes of $8 \leq n \leq 10$, in which the impurity M tends to be encapsulated at the center of the B_n rings [15–20]. For the sizes of B_n with $n > 10$, numerous geometrical patterns of boron clusters doped with a transition metal were found, such as the leaf-like, pyramid-like, umbrella-like, or metallo-borophene structures [21–23]. Remarkably, our previous study indicates that the iron-doped $B_{14}Fe$ and $B_{16}Fe$ are stabilized DR tubes, whereas $B_{18}Fe$ and $B_{20}Fe$ are stabilized fullerenes [24]. Most recently, our systematic investigation on singly and doubly nickel-doped boron clusters reveals that from the size $n = 14$, the Ni impurities cause stronger effects, and the most stable isomers B_nNi_m thus favor the shape of the related DR tubular boron structures [25]. The formation and high thermodynamic stability of boron clusters doped with both Fe and Ni certify the use of transition-metal atoms as impurities to generate various growth paths leading to larger boron clusters possessing peculiar 3D structures, such as tubes, cages, or fullerenes [26].

Although some studies on transition-metal-doped boron clusters have been carried out, the investigations on metal-doped boron clusters, in particular at the sizes $n > 10$, are insufficient. There are still some boron clusters doped with 3*d* transition metals that have not been systematically examined yet. Only a few B_nM_m clusters, with M being a transition metal, such as Sc, Ti, Fe, Co, and Ni, were reported in the recent past [25, 27, 28]. Motivated by that, we set out to operate a theoretical study on the boron clusters doped with a transition metal atom $B_{14}M$, where M is a first-row transition metal ranging from Sc to Cu, using density functional theory (DFT) calculations. We thoroughly identify the geometries of the most stable structures and, thereby, explore their exciting possibilities of structural evolution as well as determine their electronic configuration and energetic parameters.

2 Computational Methods

In consideration of the reliability tests obtained from many earlier reports on boron-based clusters [8, 24, 25, 27–29], we have used the hybrid TPSSh functional in conjunction with the 6-311+G(d) basis sets as implemented in the Gaussian 09 package [30] for all calculations in this work. The search for energy minima is conducted using two diverse approaches. First, all possible structures of B_nM_m clusters are generated using a stochastic algorithm [31]. In addition, initial structures of B_nM_m are manually composed by adding M-atoms at all possible positions on the surfaces of the known B_{14} structures. The harmonic vibrational frequencies of B_nM_m are afterward identified at the same level.

For the analysis of the electronic distribution, we use the electronic density of state (DOS) approach. The values of DOSs are also obtained using TPSSh/6-311+G(d) computations.

3 Results and discussion

3.1 Lower-lying isomers of $B_{14}M$ clusters

The shapes of the equilibrium structures of the $B_{14}M$ clusters detected, their spin states, and DFT relative energies are shown in **Fig. 1** and **Fig. 2**. Because of a large number of isomers located on the potential energy surfaces of the clusters

pISSN 1859-1388
eISSN 2615-9678

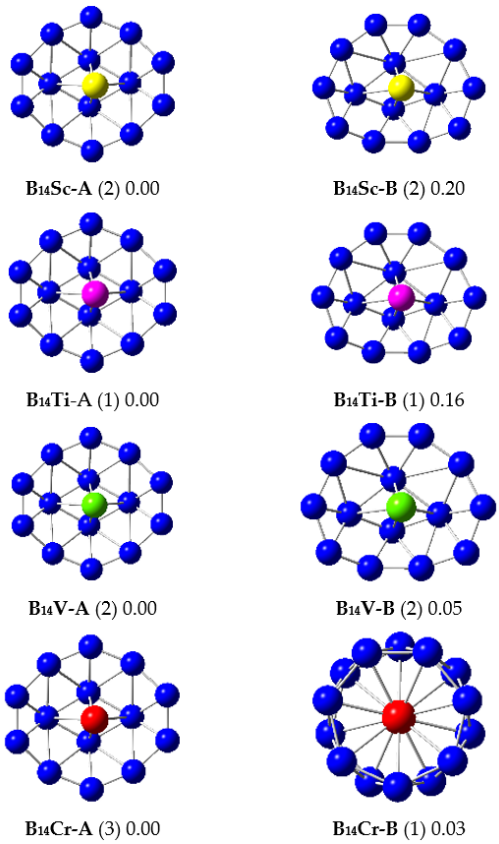

Fig. 1. Shapes, spin states (in the brackets), and relative energies (ΔE, eV) of the lower-lying isomers $B_{14}M$ with M = Sc, Ti, V, and Cr. ΔE values are obtained from TPSSh/6-311+g(d) + ZPE computations

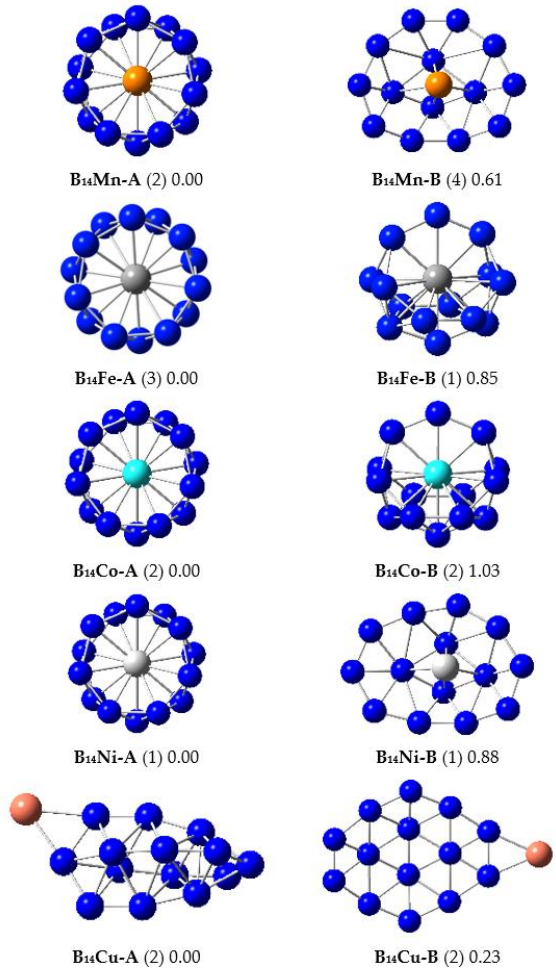

Fig. 2. Shapes, spin states (in the brackets), and relative energies (ΔE, eV) of the lower-lying isomers $B_{14}M$ with M = Mn, Fe, Co, Ni, and Cu. ΔE values are obtained from TPSSh/6-311+g(d) + ZPE computations

considered, only the ground state and the second lower-lying isomer whose relative energy is closest to the corresponding ground state isomer are presented for each size. Conventionally, a **B_{14}M-X** label is used for each isomer of the $B_{14}M$ clusters considered, where **M is Sc**, **Ti**, **V**, **Cr**, **Mn**, **Fe**, **Co**, **Ni**, and **Cu**, and **X = A** and **B** referring to the different isomers with increasing relative energy. The main geometrical characteristics can briefly be described as follows:

As M is, in turn, Sc, Ti, V, and Cr, the most stable isomers of $B_{14}M$ prefer the structure in which the dopant M is capped on the surface of the quasi-planar shape of cation B_{14}^+ [2]. DFT calculations indicate two degeneracies in energy for $B_{14}V$ and $B_{14}Cr$. Interestingly, while both **B_{14}V-A** and **B_{14}V-B**, being energetic degenerated with a gap of 0.05 eV, still have the quasi-planar shapes of the B_{14} framework, there is a structure competition at $B_{14}Cr$. Accordingly, the triplet spin state **B_{14}Cr-A** continues the quasi-planar B_{14} skeleton like the $B_{14}M$ described above, whereas the closed-shell spin state **B14Cr-B**, being only 0.03 eV higher in energy than **B_{14}Cr-A**, possesses a DR structure composed of two seven-membered rings in an anti-prism disposition [6] and a Cr atom is encapsulated at the center of the tubular.

Similar to **B14Cr-B**, the lowest-lying isomers of next $B_{14}M$ clusters with M being Mn, Fe, Co, and Ni are also generated by putting the dopant M in the center of the DR cylinder B_{14}. Among them, the triplet spin state **B_{14}Fe-A** and the closed-shell electronic configuration **B_{14}Ni-A** are reported in our previous studies [24, 25]. The remaining isomers with different geometrical structures are much less stable with a large energy gap, being at least 0.61 eV.

In the family $B_{14}M$ with M ranging from Sc to Cu, only the most stable structure of $B_{14}Cu$ keeps the fullerene-like geometry of pure neutral B_{14} [5]. The isomer **B_{14}Cu-A**, formed by adding a Cu atom on an edge of the fullerene framework B_{14}, is 0.23 eV lower in energy than **B_{14}Cu-B**, also formed by adding a Cu atom on an edge of the quasi-planar structure of B_{14}^+ [2].

Generally, the doping of B_{14} successively with different first-row transition metals ranging from Sc to Cu tends to make the DR structure, in which the metal dopant is located at the center of DR B_{14} tubular. For three lightest dopants, including Sc, Ti, and V, the DR shape has not appeared yet. For M = Cr, however, there is a structure competition because the DR structure is almost as stable as the quasi-planar structure. Subsequently, the calculated results of $B_{14}M$ with M being, in turn, Mn, Fe, Co, and Ni, show the strong domination of DR structure. It can be understood by the fact that the atomic radius of Sc, Ti, and V is longer than that of the remaining 3*d* metals. Hence, the hollow volume inside the B_{14} DR is not large enough to confine these metal impurities, whereas the heavier dopants (M = Cr, Mn, Fe, Co, and Ni) with shorter atomic radius can be encapsulated at the center of DR B_{14}. Moreover, the $B_{14}Cr$ can be considered as a "critical point" of the $B_{14}M$ series since both DR and quasi-planar shapes exist together. The $B_{14}Cu$ species is an exception because its geometrical structure is different from DR. It can be rationalized by the fact that the copper atom with $4s^13d^{10}$ electronic configuration can easily lose one valence electron to get the full-filled configuration and behaves as an electron donor. Therefore, the Cu atom favors adsorption on a bridge site of the fullerene B_{14} framework.

3.2 Relative stabilities of $B_{14}M$

Like in previous studies on various clusters [25, 32, 33], the relative stabilities of $B_{14}M$ species considered can be evaluated on the basis of the average binding energy per atom (E_b), which is conventionally defined as follows:

$$E_b(B_{14}M) = [14E(B) + E(M) - E(B_{14}M)]/15 \quad (1)$$

Furthermore, the average binding energy of pure boron neutral B_{15} with the same number of atoms is also determined for comparison with $E_b(B_{14}M)$:

$$E_b(B_{15}) = [15E(B) - E(B_{15})]/15 \quad (2)$$

where E(B) and E(M) are the total energy of the B-atom and M-atom, respectively. $E(B_{14}M)$ and $E(B_{15})$ are the total energy of the neutral $B_{14}M$ and B_{15}, respectively. All these energetic values are obtained from TPSSh/6-311+G(d) + ZPE calculations, and the values of $E(B_{14}M)$ with M being from Sc to Cu, in comparison with $E(B_{15})$, are illustrated in Fig. 3. The coordinate of the geometry of neutral B_{15} is taken from a previous study of Tai et al. [4]

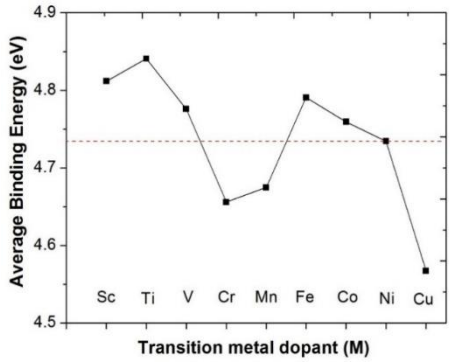

Fig. 3. Average binding energies (E_b, eV) of 3*d* transition metal doped $B_{14}M$

pISSN 1859-1388
eISSN 2615-9678

Fig. 3 shows except for the E_b values of $B_{14}Ni$ and B_{15} being almost equal, the E_b values of $B_{14}Sc$, $B_{14}Ti$, $B_{14}V$, $B_{14}Fe$, and $B_{14}Co$ species are higher than those of B_{15}, whereas the E_b values of $B_{14}Cr$, $B_{14}Mn$, and $B_{14}Cu$ are lower than those of $E_b(B_{15})$. In other words, while Sc, Ti, V, Fe, and Co dopants increase the cluster stability concerning fragmentations, Cr, Mn, and Cu tend to decrease it. In addition, when M goes successively from Sc to Cu, the $E_b(B_{14}M)$ gets the maximum value of cluster stability at $B_{14}Ti$. It decreases from $B_{14}Ti$ to $B_{14}Cr$ and then increases again from $B_{14}Cr$ to $B_{14}Fe$. From Fe to Cu, the cluster stability of $E_b(B_{14}M)$ continuously decreases. In particular, it strongly decreases from $B_{14}Ni$ to $B_{14}Cu$ and gets the smallest value at $B_{14}Cu$. This proves that Cu dopant prefers to donate electrons instead of making chemical bonds.

3.3 Density of states of $B_{14}Ti$ and $B_{14}Fe$

The picture of the binding energy of $B_{14}M$ reveals that both $B_{14}Ti$ clusters – closed-shell electronic configuration and the high spin state $B_{14}Fe$ – exhibit the enhanced thermodynamic stability with higher average binding energies. They have typical geometric structures, in which the Ti dopant is capped on the surface of the quasi-planar B_{14}, whereas the Fe dopant is located at the center of a B_{14} DR. To achieve more insights into the relative stability of the clusters considered, we now examine their molecular orbital pictures under the viewpoints of the jellium shell model [34], in which the total density of states of a molecular system can be considered as an energy spectrum of its molecular orbitals (MOs), whereas the partial density of states (pDOS) is figured out only from relevant atomic orbitals and thereby shows the composition of the MOs involved.

Fig. 4 shows both partial and total densities of states of the singlet $B_{14}Ti$-A and the triplet DR $B_{14}Fe$-A, in which the α and β spin MOs are separately plotted. This interprets a clear picture of

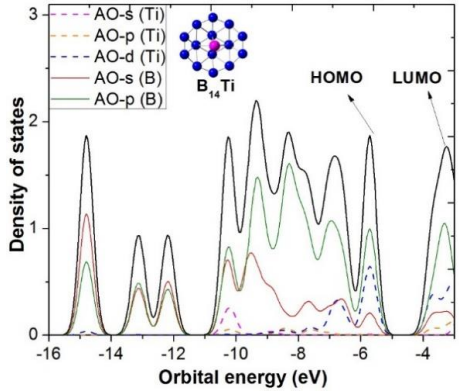

a) Total (DOS) and partial (pDOS) of $B_{14}Ti$

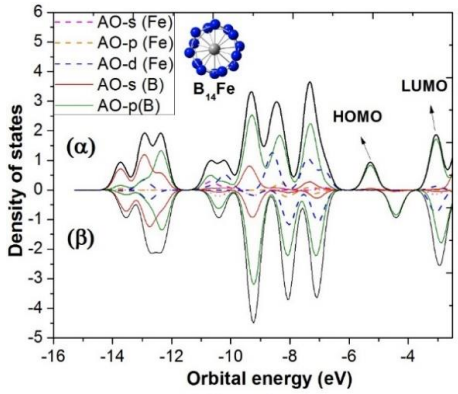

b) Total (DOS) and partial (pDOS) of $B_{14}Fe$

Fig. 4. Total (DOS) and partial (pDOS) densities of state of (a) $B_{14}Ti$ and (b) $B_{14}Fe$

their electronic shells. As expected, the frontier MOs are composed mainly of the 2p(B) and 3d AOs of Ti or Fe dopant but with a larger component of the boron AOs. The HOMO and LUMO of $B_{14}Fe$, however, appear particularly from the boron AOs, whereas the HOMO and LUMO of $B_{14}Ti$ are composed predominantly of 2p(B), 3d(Ti), and, to a lesser extent, of 2s(B) AOs.

4 Concluding Remarks

In this investigation, both geometrical and electronic structures of the first-row-transition-metal-doped boron $B_{14}M$ clusters, where M is, in turn, Sc, Ti, V, Cr, Mn, Fe, Co, Ni, and Cu in the neutral state, were examined using the quantum

chemical DFT approach. The clusters with lighter dopants (M = Sc, Ti, and V) prefer the capped quasi-planar structure, while the heavier ones (M = Cr, Mn, Fe, Co, and Ni) favor a DR structure, in which the metal dopant is located at the center of the DR B_{14} tubular. The cluster $B_{14}Cr$ can be considered as a critical point due to the structure competition between endohedrally doped DR and exohedrally capped quasi-planar structure. The $B_{14}Cu$, which is formed by adding the Cu dopant on an edge of the fullerene B_{14}, is an exception. The results also indicate that besides the typical geometric features, both $B_{14}Ti$ and $B_{14}Fe$ species have enhanced thermodynamic stabilities with high average binding energies. Their MO properties, thus, are examined from the density of state approaches.

Acknowledgements

This research was supported by Vietnam's National Foundation for Science and Technology Development (NAFOSTED) under Grant No. 104.06-2015.71.

References

1. Tai TB, Tam NM, Nguyen MT. The Boron conundrum: the case of cationic clusters Bn+with n = 2–20. Theoretical Chemistry Accounts. 2012;131(6):1241.
2. Tai TB, Tam NM, Nguyen MT. The Boron conundrum: the case of cationic clusters Bn+with n = 2–20. Theoretical Chemistry Accounts. 2012;131(6):1241.
3. Sergeeva AP, Popov IA, Piazza ZA, Li W-L, Romanescu C, Wang L-S, et al. Understanding Boron through Size-Selected Clusters: Structure, Chemical Bonding, and Fluxionality. Accounts of Chemical Research. 2014;47(4):1349-58.
4. Tai TB, Tam NM, Nguyen MT. Structure of boron clusters revisited, Bn with n = 14–20. Chemical Physics Letters. 2012;530:71-6.
5. Cheng L. B14: An all-boron fullerene. The Journal of Chemical Physics. 2012;136(10):104301.
6. Yuan Y, Cheng L. B142+: A magic number double-ring cluster. The Journal of Chemical Physics. 2012;137(4):044308.
7. Kiran B, Bulusu S, Zhai H-J, Yoo S, Zeng XC, Wang L-S. Planar-to-tubular structural transition in boron clusters: B₂₀ as the embryo of single-walled boron nanotubes. Proceedings of the National Academy of Sciences of the United States of America. 2005;102(4):961.
8. Pham HT, Duong LV, Pham BQ, Nguyen MT. The 2D-to-3D geometry hopping in small boron clusters: The charge effect. Chemical Physics Letters. 2013;577:32-7.
9. Chacko S, Kanhere DG, Boustani I. Ab initio density functional investigation of ${\mathrm{B}}_{24}$ clusters: Rings, tubes, planes, and cages. Physical Review B. 2003;68(3):035414.
10. Pham HT, Duong LV, Nguyen MT. Electronic Structure and Chemical Bonding in the Double Ring Tubular Boron Clusters. The Journal of Physical Chemistry C. 2014;118(41):24181-7.
11. Johansson MP. On the Strong Ring Currents in B20 and Neighboring Boron Toroids. The Journal of Physical Chemistry C. 2009;113(2):524-30.
12. Bean DE, Fowler PW. Double Aromaticity in "Boron Toroids". The Journal of Physical Chemistry C. 2009;113(35):15569-75.
13. Janssens E, Neukermans S, Nguyen HMT, Nguyen MT, Lievens P. Quenching of the Magnetic Moment of a Transition Metal Dopant in Silver Clusters. Physical Review Letters. 2005;94(11):113401.
14. Ngan VT, Janssens E, Claes P, Fielicke A, Nguyen MT, Lievens P. Nature of the interaction between rare gas atoms and transition metal doped silicon clusters: the role of shielding effects. Physical Chemistry Chemical Physics. 2015;17(27):17584-91.
15. Romanescu C, Galeev TR, Li W-L, Boldyrev AI, Wang L-S. Transition-Metal-Centered Monocyclic Boron Wheel Clusters (M©Bn): A New Class of Aromatic Borometallic Compounds. Accounts of Chemical Research. 2013;46(2):350-8.
16. Romanescu C, Galeev TR, Li W-L, Boldyrev AI, Wang L-S. Geometric and electronic factors in the rational design of transition-metal-centered boron molecular wheels. The Journal of Chemical Physics. 2013;138(13):134315.
17. Galeev TR, Romanescu C, Li W-L, Wang L-S, Boldyrev AI. Observation of the Highest Coordination Number in Planar Species: Decacoordinated Ta©B10− and Nb©B10− Anions.

pISSN 1859-1388
eISSN 2615-9678

Angewandte Chemie International Edition. 2012;51(9):2101-5.

18. Romanescu C, Galeev TR, Li W-L, Boldyrev AI, Wang L-S. Aromatic Metal-Centered Monocyclic Boron Rings: Co©B8− and Ru©B9−. Angewandte Chemie International Edition. 2011;50(40):9334-7.
19. Li W-L, Romanescu C, Galeev TR, Piazza ZA, Boldyrev AI, Wang L-S. Transition-Metal-Centered Nine-Membered Boron Rings: M©B9 and M©B9– (M = Rh, Ir). Journal of the American Chemical Society. 2012;134(1):165-8.
20. Li W-L, Ivanov AS, Federič J, Romanescu C, Černušák I, Boldyrev AI, et al. On the way to the highest coordination number in the planar metal-centred aromatic Ta©B10− cluster: Evolution of the structures of TaBn− (n = 3–8). The Journal of Chemical Physics. 2013;139(10):104312.
21. Liao Y, Cruz CL, von Ragué Schleyer P, Chen Z. Many M©Bn boron wheels are local, but not global minima. Physical Chemistry Chemical Physics. 2012;14(43):14898-904.
22. Li W-L, Romanescu C, Piazza ZA, Wang L-S. Geometrical requirements for transition-metal-centered aromatic boron wheels: the case of VB10−. Physical Chemistry Chemical Physics. 2012;14(39):13663-9.
23. Li W-L, Jian T, Chen X, Chen T-T, Lopez GV, Li J, et al. The Planar CoB18− Cluster as a Motif for Metallo-Borophenes. Angewandte Chemie International Edition. 2016;55(26):7358-63.
24. Tam NM, Pham HT, Duong LV, Pham-Ho MP, Nguyen MT. Fullerene-like boron clusters stabilized by an endohedrally doped iron atom: BnFe with n = 14, 16, 18 and 20. Physical Chemistry Chemical Physics. 2015;17(5):3000-3.
25. Tam NM, Duong LV, Pham HT, Nguyen MT, Pham-Ho MP. Effects of single and double nickel doping on boron clusters: stabilization of tubular structures in BnNim, n = 2–22, m = 1, 2. Physical Chemistry Chemical Physics. 2019;21(16):8365-75.
26. Shakerzadeh E, Van Duong L, Tahmasebi E, Nguyen MT. The scandium doped boron cluster B27Sc2+: a fruit can-like structure. Physical Chemistry Chemical Physics. 2019;21(17):8933-9.
27. Pham HT, Nguyen MT. Effects of bimetallic doping on small cyclic and tubular boron clusters: B7M2 and B14M2 structures with M = Fe, Co. Physical Chemistry Chemical Physics. 2015;17(26):17335-45.
28. Pham HT, Tam NM, Pham-Ho MP, Nguyen MT. Stability and bonding of the multiply coordinated bimetallic boron cycles: B8M22−, B7NM2 and B6C2M2 with M = Sc and Ti. RSC Advances. 2016;6(57):51503-12.
29. Duong LV, Pham HT, Tam NM, Nguyen MT. A particle on a hollow cylinder: the triple ring tubular cluster B27+. Physical Chemistry Chemical Physics. 2014;16(36):19470-8.
30. Frisch MJ, Schlegel HB, Scuseria GE, Robb MA, Cheeseman JR, Montgomery JA, et al. Gaussian 09 Revision: D.01, Gaussian Inc., Wallingford, CT, USA. Gaussian 09 Revision: D01. 2009.
31. Tai TB, Nguyen MT. A Stochastic Search for the Structures of Small Germanium Clusters and Their Anions: Enhanced Stability by Spherical Aromaticity of the Ge10 and Ge122− Systems. Journal of Chemical Theory and Computation. 2011;7(4):1119-30.
32. Pham HT, Cuong NT, Tam NM, Tung NT. A Systematic Investigation on CrCun Clusters with n = 9–16: Noble Gas and Tunable Magnetic Property. The Journal of Physical Chemistry A. 2016;120(37):7335-43.
33. Tam NM, Tai TB, Ngan VT, Nguyen MT. Structure, Thermochemical Properties, and Growth Sequence of Aluminum-Doped Silicon Clusters SinAlm (n = 1–11, m = 1–2) and Their Anions. The Journal of Physical Chemistry A. 2013;117(31):6867-82.
34. Brack M. The physics of simple metal clusters: self-consistent jellium model and semiclassical approaches. Reviews of Modern Physics. 1993;65(3):677-732.